Silicon Photonic Tunable Flat-top Filters based on CROW Structures at 2-μm Spectral Range

You Wu[1], Xiaoyuan Guo[1], Xi Wang[1], Jiangbing Du[2], Qinghai Song[3], and Ke Xu[1, *]
[1]*Department of Electronic and Information Engineering, Harbin Institute of Technology, Shenzhen 518055, China*
[2]*State Key Laboratory of Advanced Optical Communication Systems and Networks, Shanghai Jiao Tong University, Shanghai 200240, China*
[3]*Department of Science, Harbin Institute of Technology, Shenzhen 518055, China*
* *kxu@hit.edu.cn*

Abstract: Silicon photonic tunable flat-top filters are demonstrated via the 5th-order and the 10th-order CROW structure at 2-μm waveband. Box-like transmission spectra are measured with 3-dB bandwidth of 3.34 nm and 5.34 nm, respectively. © 2022 The Author(s)

1. Introduction

To meet increasing demands for optical fiber communication bandwidth, seeking for broader communication window is of great research interest. The emerging waveband at 2-μm wavelength has been expected to accommodate more data channels since the thulium doped fiber has >30 THz gain bandwidth [1]. The fiber attenuation at this waveband is also predicted to be as low as 0.1 dB [2]. Single-lane transmission with 100 Gbit/s direct detection and 76.56 Gbit/s with coherent detection have been achieved at 2-μm wavelengths [3, 4]. Various silicon photonic devices have been demonstrated at 2-μm including modulators [5, 6] photodetectors [7], splitters [8], and so forth. Optical filters have also been implemented by micro rings [9], arrayed waveguide gratings [10], and Bragg gratings [11]. More recently, cascaded interferometers are demonstrated for flat-top filters on silicon platforms [12]. But the passband is too wide and the device occupied too much chip area.

In this work, we demonstrate narrowband flat-top and tunable optical filters on silicon platform based on coupled resonator optical waveguides (CROW) structure at 2-μm. The transmission spectra have excellent shape factor and flatness. These features are highly desirable in fiber communication systems. The devices are fully compatible with standard silicon photonic fabrication.

2. Devices Design and Fabrication

The devices were designed on silicon-on-insulator (SOI) platform with 220 nm top silicon and 2 μm buried oxide. Both the the 5th-order filter and the 10th-order filter have the same bending radius of 9 μm and strip width of 670 nm to accommodate the fundamental mode at 2-μm. The waveguide is fully etched with 220 nm depth to minimize the bending loss. The electrodes made of TiN are designed to be 120 nm high and 1.1 μm wide, covering the half-perimeter length of the racetrack area. The transfer matrix method is employed to calculate and determine the optimal gap between different coupling waveguides to achieve a preferable spectral response. To enhance the coupling, race track resonator was designed with a coupling length of 12.5 μm and a gap width of 0.23 μm.

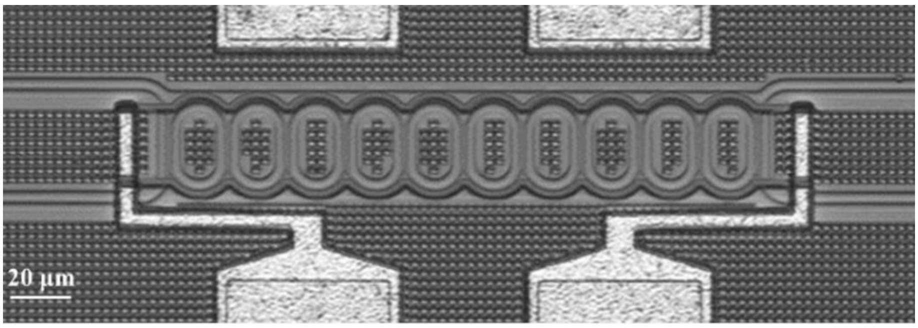

Fig. 1. The microscope image of the fabricated the 10th-order filter.

The devices were fabricated via standard silicon photonic multi-project-wafer shuttle run offered by CUMEC. Both the 5th-order filter and the 10th-order filter based on CROW structure were designed and fabricated on the same SOI wafer to experimentally characterize and compare the filtering performance. The microscope image of the the 10th-order filter is shown in Fig. 1. The heaters were also designed and fabricated using TiN metal strip to align the resonance wavelengths of different resonators via thermo-optic effect.

3. Experimental Results

The tunable laser OETLS-300-2000 was used as the source, and an optical power meter (OPM) was applied to measure the transmitted optical power at the drop port. Thulium doped fiber amplifier (TDFA) was utilized to measure zoom-up spectra of both filters, because the detection limit is constrained by the OPM. The full spectra were measured without TDFA, which is subject to limitation on its narrow bandwidth. Grating couplers were used to interface the silicon waveguide device and the jump fibers. The coupling loss is measured to be 8 dB/facet. The measured transmission results were normalized with respect to a pair of back-to-back grating couplers connected by a straight single-mode waveguide on the same chip. The coupling loss can be further improved by apodizing the grating period to match the mode profile The tuning experiment was also carried out on the the 10th-order filter with a direct current source (Keithley 2450). Electrical power of 0 mW, 10 mW, 20 mW, and 40 mW were applied in this experiment.

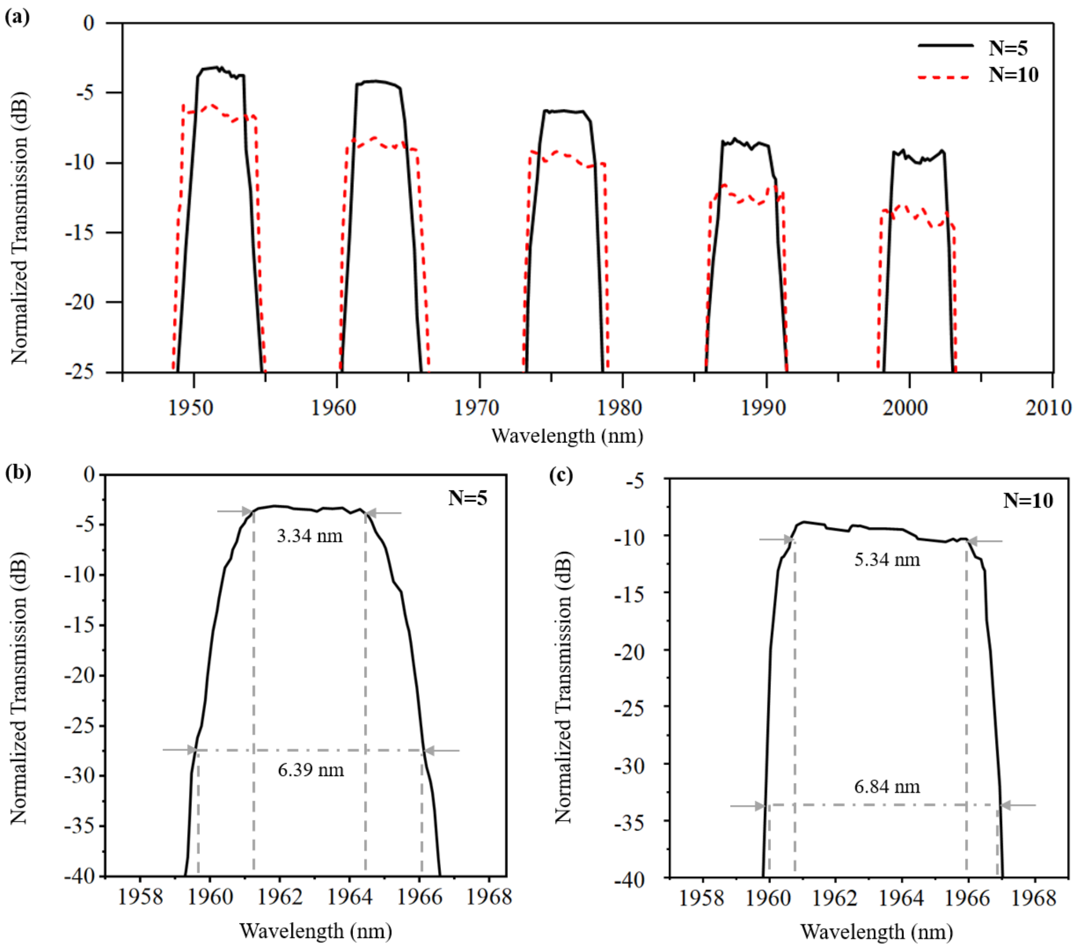

Fig. 2. (a) The transmission spectra of both the 5th-order andthe 10th-order filters. The zoom-up resonance spectrum of (b) the 5th-order and (c) the 10th-order filter at the central wavelength 1963 nm.

Fig. 2 (a) shows the normalized transmission responses at the drop port of the fabricated devices of the 5th-order and the 10th-order. The result suggested that the free spectral ranges (FSR) of both components are 12.3 nm. It can be seen that box-like spectrum shapes has been achieved at 2-µm waveband by the designed CROWs. Also, it is obvious that the the 10th-order filter has broader bandwidth but suffers higher loss due to the transmission through more cascaded ring resonators. Due to the detection limit, we are not able to measure the noise floor. The zoom-up spectral responses of the filters from 1958 nm to 1968 nm are measured by scanning the wavelengths with finer resolution, as shown in Fig. 2 (b) and Fig. 2 (c). The 3-dB bandwidths of the the 5th-order filter and the the 10th-order filter are measured to be 3.34 nm and 5.34 nm. The 25-dB bandwidth is estimated to be 6.39 nm and 6.84 nm, respectively. Besides, the shape factor at 25-dB/3-dB of the the 5th-order filter is 0.52, while the same figure up to 0.78 can be achieved by the the 10th-order filter. Accordingly, the box-like response can be preferably achieved via a higher-order filter. In addition, it can be seen that both the 5th-order and the 10th-order filter obtain an extinction ratio (ER) over 35 dB. Moreover, the the 10th-order filter is expected to gain an ultra-high ER over 100 dB. The the 10th-order filter also has a steep sideband with the slope of 27.3 dB/nm and can repress crosstalk. In conclusion, high order microring filter can achieve a well box-like transmission response with high shape factor, ER, and steep sideband, but the order should not be too high in compromising of the footprint and the loss.

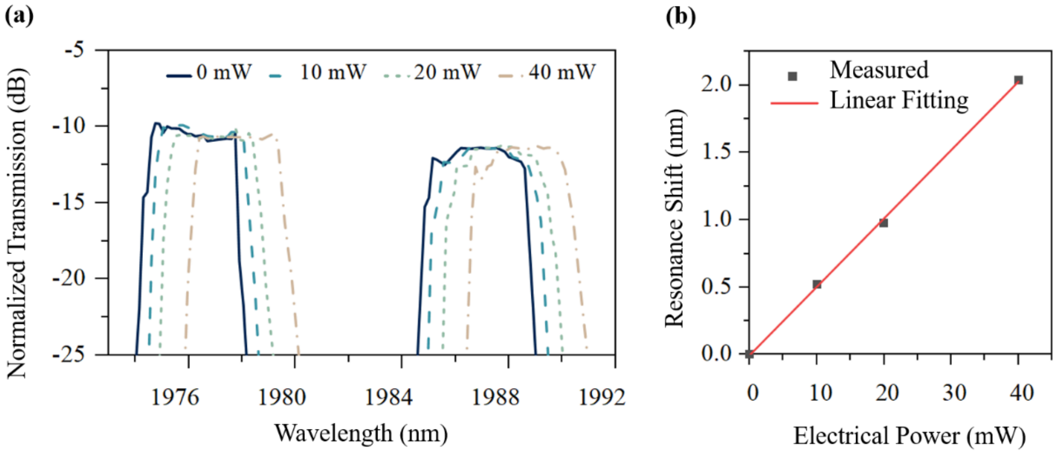

Fig. 3. (a) Measured spectral responses of the 10th–order filter under tuning with different electrical power. (b) The resonance shift as a function of the consumed electrical power.

The results of the thermal tuning experiment are illustrated in Fig. 3. The transmission spectral response from 1974 nm to 1992 nm is measured under different applied powers and is shown in Fig. 3 (a). It can be seen that the heating effect increases the refractive index and hence induces the spectrum red shift. Fig. 3 (b) indicates the resonance shift as a function of the consumed electrical power. The linear regression method is utilized to fit the curve, proving that the central wavelength can be tuned with an efficiency of 0.051 nm/mW.

4. Conclusion

We have demonstrated a tunable cascaded micro ring filter based on CROW structure at 2-µm with box-like transmission spectrum and broad 3-dB bandwidth. Both the 5th-order filter and the 10th-order filter were fabricated. The two filters have 3-dB bandwidth of 3.34 nm, 5.34 nm, and shape factor of 0.52, 0.78 respectively. The thermal tuning efficiency of the the 10th-order filter is 0.051 nm/mW. This work show that the CROW filter can provide flat-top transmission response at 2-µm.

Acknowledgement

This research was funded by National Natural Science Foundation of China (61875049, U21A20454, 61875124, 61935011), Science, Technology and Innovation Commission of Shenzhen Municipality (RCYX20210609103707009, JCYJ20180507183418012), Natural Science Foundation of Guangdong Province for Distinguished Young Scholars (2022B1515020057) and Fundamental Research Funds for the Central Universities (Grant No. HIT.BRET. 2022012).

5. References

[1] Z. Li, et al, "Thulium-doped fiber amplifier for optical communications at 2 µm," Opt. Express 21, 9289-9297 (2013).
[2] P. J. Roberts, et al, "Ultimate low loss of hollow-core photonic crystal fibers," Opt. Express 13, 236-244 (2005).
[3] W. Shen, et al, "100-Gbps 100-m hollow-core fiber optical interconnection at 2-micron waveband by PS-DMT," in Optical Fiber Communication Conference (OFC) 2020, OSA Technical Digest (Optica Publishing Group, 2020), paper Th2A.1.
[4] D. Kong, et al, "Super-broadband on-chip continuous spectral translation unlocking coherent optical communications beyond conventional telecom bands," Nat. Commun. 13, 4139 (2022).
[5] W. Cao, et al, "High-speed silicon modulators for the 2 µm wavelength band." Optica 5, 1055-1062 (2018).
[6] X. Wang, et al, "High-speed silicon photonic Mach–Zehnder modulator at 2 µm," Photonics. Res. 9, 535-540 (2021).
[7] S. Xu, et al, "High-speed photo detection at two-micron-wavelength: technology enablement by GeSn/Ge multiple-quantum-well photodiode on 300 mm Si substrate," Opt. Express 27, 5798-5813 (2019).
[8] Z. Wang, et al, "Ultra-compact and broadband 3-dB power splitter based on subwavelength grating at 2-µm," in Optical Fiber Communication Conference (OFC) 2021, OSA Technical Digest (Optica Publishing Group, 2021), paper Tu1C.5.
[9] J. Li, et al, "2-µm Wavelength grating coupler, bent waveguide, and tunable microring on silicon photonic MPW," IEEE Photon. Technol. Lett. 30, 471-474 (2018).
[10] Y. Liu, et al, "Silicon photonic arrayed waveguide grating with 64 channels for the 2 µm spectral range," Opt. Lett. 47, 1186-1189 (2022).
[11] D. Liu, et al, "Silicon multimode waveguide grating filter at 2 µm," J. Lightwave Technol. 37, 2217-2222 (2019).
[12] Q. Yi, et al, "Silicon photonic flat-top WDM (de)multiplexer based on cascaded Mach-Zehnder interferometers for the 2 µm wavelength band," Opt. Express 30, 28232-28241 (2022).